Available online at www.sciencedirect.com
SciVerse ScienceDirect
Journal of the European Ceramic Society xxx (2012) xxx–xxx
www.elsevier.com/locate/jeurceramsoc

Dehydroxylation of hydroxyapatite in dense bulk ceramics sintered by spark plasma sintering

Yi Liu [a,b], Zhijian Shen [a,*]

[a] *Department of Materials and Environmental Chemistry, Arrhenius Laboratory, Stockholm University, S-106 91 Stockholm, Sweden*
[b] *State Key Laboratory for Mechanical Behaviour of Materials, Xi'an Jiaotong University, 710049 Xi'an, PR China*

Abstract

Dense transparent hydroxyapatite (HAp) nanoceramic samples were prepared by spark plasma sintering of a commercial available granulated nanopowder. This made it possible for investigating the dehydroxylation behaviours of HAp in fully dense bulks. Post-SPS thermal annealing was performed in a temperature interval of 800 to 1100 °C in air. The phase analysis and microstructural characterization revealed that the dehydroxylation in fully dense HAp was initiated above 900 °C and its kinetics seems to be determined by the water vapour diffusion. Accordingly, a gradient structure consisting of porous interiors and a peculiar surface topography reflecting the water vapour escaping patterns were observed in samples experienced severe dehydroxylation.

Keywords: Bioceramics; Hydroxyapatite; Dehydroxylation; Microstructure

1. Introduction

Having good biocompatibility with human body hydroxyapatite ceramics, HAp, are ideal candidates for the replacement of damaged hard tissues, i.e. bone and teeth.[1,2] However, the applications of single phase HAp in clinic are rather limited due to its poor mechanical properties. New strategies have been developed accordingly to overcome these drawbacks. For example, HAp has been used as coatings on the metal substrate or as fillers in the bio-inert ceramic matrix.[3,4] Another strategy to improve the mechanical properties of HAp ceramics is to add a second-phase for reinforcement.[5–7] In all these approaches, the thermal stability of HAp has been a major concern. Once decomposition takes place during thermal processing of HAp, the physical, chemical, mechanical and biological properties of HAp will be affected.[8]

The dehydroxylation of HAp takes place ahead of the decomposition that occurs at a higher temperature. Dehydroxylation yields the formation of hydroxyoxyapatite (OHAp) and oxyapatite (OAp),[8–10] whereas decomposition gives rise to tricalcium phosphate (TCP) and tetracalcium phosphate (TTCP)[8,11–14] by following the equation 1 listed below.

$$\mathrm{HAp} \rightarrow \mathrm{OHAp} \rightarrow \mathrm{OAp} \rightarrow \mathrm{TCP} + \mathrm{TTCP} \quad (1)$$

These compounds show higher solubility than HAp in aqueous environment,[15] which deteriorates the chemical stability and mechanical properties but enhance in vivo degradation of the HAp products. Therefore, in order to get the dense HAp ceramic or its composite without decomposition, low sintering temperatures have to be applied. So far, this goal has been achieved by two-step sintering,[16] morphology enhanced sintering,[17] microwave sintering,[18,19] hot pressing[20] or spark plasma sintering (SPS).[5,21] In all these processes the dehydroxylation of HAp has not been totally avoided, as it starts already at about 800 °C[12,22] or even lower,[9,10] a temperature lower or very close to the applied sintering temperature.

As known, dehydroxylation occurring during the sintering is a dynamic process determined by the water vapour releasing speed, which in turn depends on the microstructure developed. In sintered bodies with close pores the water vapour releasing from the dehydroxylation will be trapped inside the close pores. A local hydrothermal environment is accordingly established inside these pores filled with high pressure steam, which will influence the sintering and grain growth behaviour of HAp. Even before the total isolation of the pores, the atomic diffusion

* Corresponding author. Tel.: +46 8 16 3568; fax: +46 8 15 2187.
E-mail address: shen@mmk.su.se (Z. Shen).

0955-2219/$ – see front matter © 2012 Elsevier Ltd. All rights reserved.
doi:10.1016/j.jeurceramsoc.2012.02.025

responsible for densification may also be influenced because of the steam flows inside the sintering compact. However, investigations on the dehydroxylation behaviour of HAp ceramics have only been focused on the kinetic processes until now.[8,10] No work has been done to study the effect of dehydroxylation on the microstructure evolution.

In the present work, fully dense transparent HAp ceramics were firstly prepared by spark plasma sintering, SPS, at a minimized temperature by applying a high heating rate and a short holding time. The as prepared HAp ceramics are almost free from dehydroxylation. This makes it possible for us to follow the dehydroxylation process in fully dense ceramics and study its effect on the microstructure evolution by post-SPS thermal annealing in air.

2. Experimental

2.1. Spark plasma sintering

Commercially available granulated HAp nanopowders (PLASMA BIOTAL Ltd) were directly used for SPS without any treatment. 0.6 g powders were loaded into a graphite die with an inner diameter of 12 mm and then the sintering was carried out in an SPS apparatus (Sumitomo Coal Mining Co., Japan) in the vacuum of 4 Pa. The temperature was measured by an infrared pyrometer that was focused on the surface of the graphite die. The transparent HAp ceramics were sintered at 925 °C for 3 min under a uniaxial pressure of 100 MPa. After sintering, the samples were grinded and polished down to 1 μm surface finishing.

2.2. Post-SPS thermal annealing in air

Each polished transparent HAp ceramic sample was cut into four small pieces. A single piece was used in each thermal annealing test conducted in the ambient air within the temperature range of 800–1100 °C with an interval of 100 °C. The samples were heated to 700 °C at a heating rate of 10 °C/min and then a heating rate of 2 °C/min was adopted until the final temperature. After reaching the final temperature, the power of the furnace was turned off and the samples were cooled down rapidly as the furnace cooling. We chose to not apply any holding in order to follow a continuous microstructure evolution when the annealing temperature linearly increased from 800 °C to 1100 °C.

2.3. Characterizations

Density was measured using the Archimedes' principle. Each sample was measured three times and the mean value is presented. Relative densities (RD) were calculated by assuming the theoretical density of HAp to be 3.156 g/cm^3.

Powder X-ray diffraction (XRD) technique was used to identify the phase transformation of the samples sintered at different temperatures. The XRD data were collected by a PANnalytical X'Pert instrument using Cu$K_{\alpha 1}$ radiation over a 2θ range of 20–55° at a step size of 0.02°. Fourier-transform infrared spectrometry (FTIR) spectroscopic measurements were carried out from 4000 to 400 cm^{-1} using a spectrometer (FTIR Varian 670-IR) equipped with a single-reflection Golden Gate ATR accessory with a diamond ATR element. The FTIR spectrum was used to estimate the dehydroxylation in connection with the thermal histories. For the sake of comparison, the spectrums were normalized using the $\nu 4$ band of the phosphate group at 600 cm^{-1} as outlined in Ref.[23]

Microstructural observations of all the samples were conducted using a field emission scanning electron microscope (FE-SEM, JSM-7000F, JEOL, Tokyo, Japan). For the thermal annealed samples, both fresh surfaces and fractural surfaces paralleled to the direction of pressure were observed. Prior to examination, the samples were carbon-coated to prevent charging in the electron microscope. In order to check the possible pores inside the transparent HAp ceramic, the transmission electron microscope (JSM-2100, JEOL, Tokyo, Japan) was employed.

3. Results and discussions

3.1. Fully dense transparent HAp ceramics with stoichiometric composition

Fig. 1(a) shows a photo of the dense HAp ceramic sample prepared by SPS at 925 °C under a uniaxial pressure of 100 MPa. The apparent high transparency indicates that the density of the prepared HAp ceramic is sufficient high, which agrees well with the result of measured RD of 99.8%. TEM investigation was performed to check the possible presence of any residual pores and the grain size. One image from this study is presented in Fig. 1(b). It clearly reveals that no pores can be found along the grain boundary or inside the grains. Furthermore, it appears that the entire view of microstructure shows a homogeneous distribution of grains with a mean size of about 100 nm. It can thus be concluded the high density and small grain size are responsible for achieved high optical transparency.

In order to examine the possible phase changes during SPS, the XRD and FTIR were conducted. The obtained XRD pattern and IR spectrum are shown in Fig. 2. It is obvious that all the XRD peaks belong to the HAp phase. No any other phases such as TCP, TTCP or CaO can be found, which indicates that decomposition did not occur when sintered at 925 °C by SPS. The absorbance peaks at 629 cm^{-1} and 3569 cm^{-1} in IR spectrum ascribes to the OH bond in HAp lattice. The presence of these two peaks gives the possibility to study the dehydroxylation in the next thermal annealing.

3.2. Density decrease accompanied with no weight loss during thermal annealing

Fig. 3 shows the variation of sample density with the annealing temperature. It appears that the relative density starts to decrease when annealed at 900 °C and shows a rapid drop at 1000 °C. This variation of densities is also associated with a change in sample colour, see Fig. 4. It is evident that the transparency of the sample was deteriorated by annealing above

Please cite this article in press as: Liu Y, Shen Z. Dehydroxylation of hydroxyapatite in dense bulk ceramics sintered by spark plasma sintering. *J. Eur. Ceram. Soc.* (2012), doi:10.1016/j.jeurceramsoc.2012.02.025

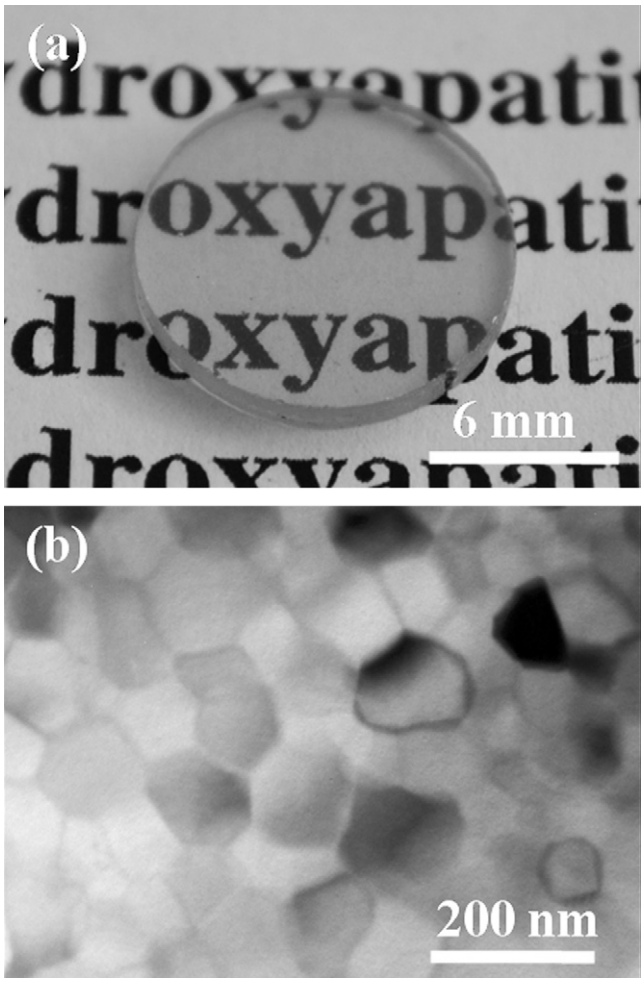

Fig. 1. Transparent HAp ceramic sintered at 925 oC. (a) Optical and (b) TEM images.

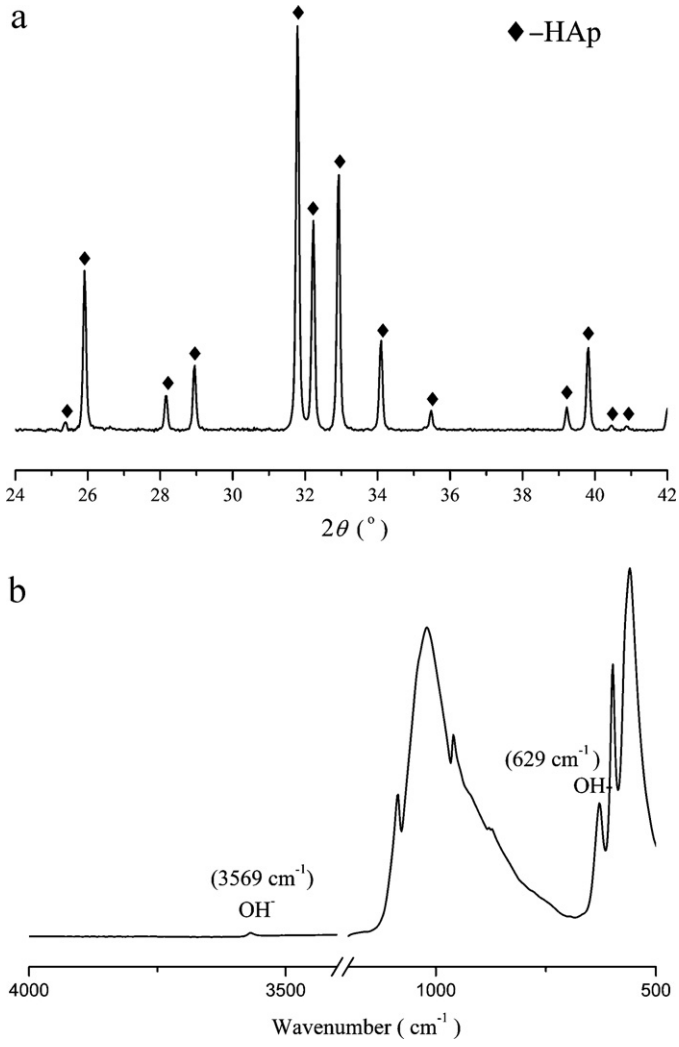

Fig. 2. Phase identification of transparent HAp ceramic. (a) XRD and (b) FTIR.

900 °C and was totally lost as the annealing temperature reached 1000 °C. Table 1 summarizes the masses of the samples before and after annealing at different temperature. No obvious weight loss can be detected accompanied with a distinct decrease of density. This fact indicates that the volume of the sample increases by annealing.

During the thermal annealing, both dehydroxylation and decomposition may result in the volume expansion. Therefore, it is necessary to examine the phase changes. Fig. 5 shows the XRD patterns and IR spectra of the samples after annealing at different temperatures. It is obvious that no differences can be distinguished between the XRD patterns before and after annealing at the temperatures interval between 800 and 1100 °C. It

Table 1
Weight changes before and after thermal annealing.

Temperature (°C)	Weight before annealing (g)	Weight after annealing (g)	ΔW (g)
800	0.1487	0.1486	0.0001
900	0.1497	0.1497	0
1000	0.1395	0.1394	0.0001
1100	0.1571	0.1569	0.0002

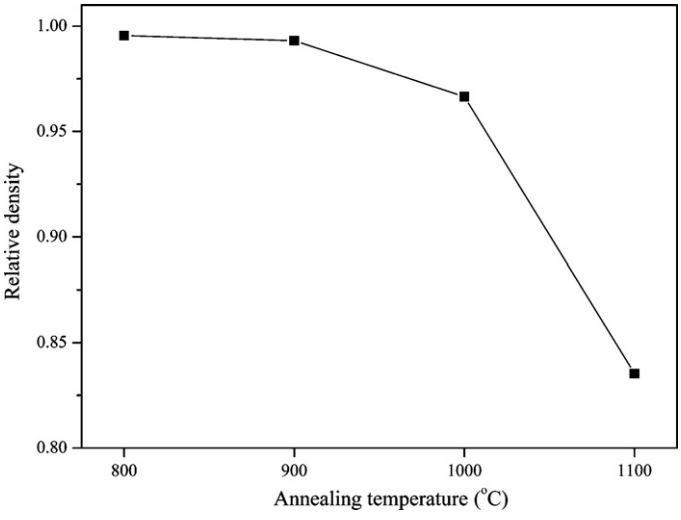

Fig. 3. Density variation after thermal annealing at different temperatures.

Please cite this article in press as: Liu Y, Shen Z. Dehydroxylation of hydroxyapatite in dense bulk ceramics sintered by spark plasma sintering. *J. Eur. Ceram. Soc.* (2012), doi:10.1016/j.jeurceramsoc.2012.02.025

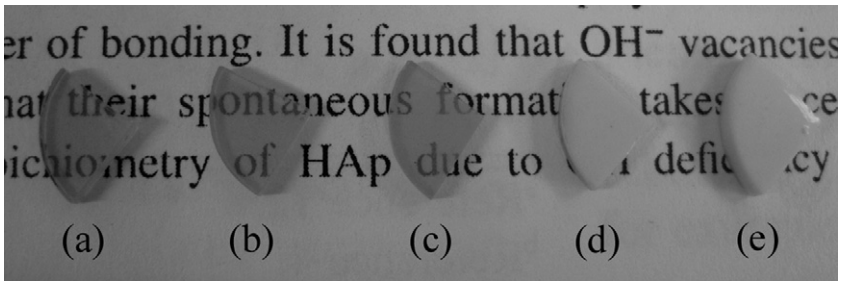

Fig. 4. Optical photos before (a) and after annealing at (b) 800 °C, (c) 900 °C, (d) 1000 °C and (e) 1100 °C.

reveals that decomposition does not occur. It seems that during thermal annealing dehydroxylation does not take place as well, because the absorbance bands of O–H bond at 629 cm^{-1} and 3569 cm^{-1} are always present and show no decrease with the increase of the annealing temperature. It is, however, worth to mention that the samples used for thermal annealing in this study are all fully dense. This means that the water vapour releasing from the dehydroxylation, if formed, will be trapped inside the sample during annealing. The trapped water vapour is able to be taken up by the HAp lattice during cooling due to the reversibility of dehydroxylation reaction. Therefore, the OH content in the annealed samples may exhibit no change, as seen in Fig. 5(b).

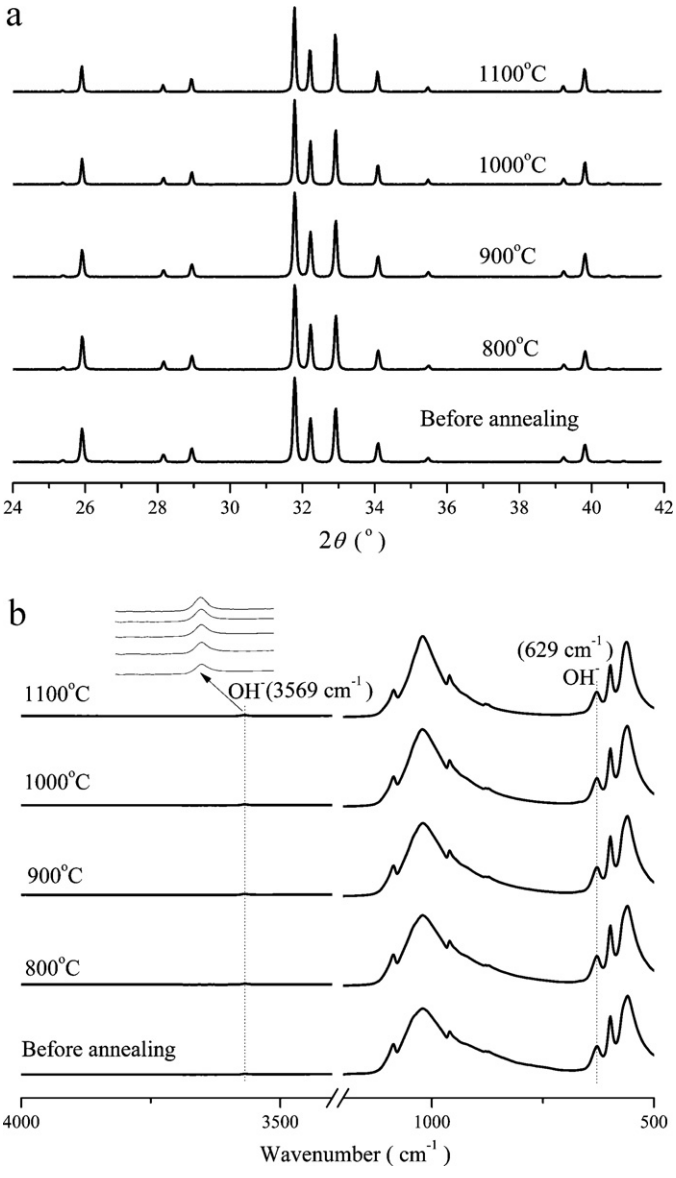

Fig. 5. Phase characterization after thermal annealing at different temperatures. (a) XRD and (b) FTIR.

3.3. *In situ formed porosity in HAp ceramics during thermal annealing*

In fact, it is hard to draw any concrete conclusion about OH content by comparing merely the peak intensity of the absorbance band of O–H bond of the samples after annealing at different temperatures. A relative content of OH can be estimated, however, by comparing of the peak intensity of OH with that of PO_4^{3-}, as summarized in Table 2. Although the normalized values are quite similar, a tendency of slight decrease of OH content is visible with the increase of annealing temperature. This indicates that the dehydroxylation does occur during the annealing. The slight decrease of OH content may attribute to the water loss near the surface part of the annealed samples. As mentioned above, if the dehydroxylation takes place inside a fully dense HAp ceramic sample, the water vapour most probably will be trapped inside the sample. However, the water vapour releasing from the dehydroxylation near the surface is easy to diffuse out during thermal annealing, leading to a slight decrease of OH content.

Fig. 6 shows the microstructures inside the samples annealed at the temperature interval of 800–1100 °C. It can be observed that a small number of very fine and isolated pores are formed by annealing at 900 °C. With the increase of the annealing temperature the pores become bigger and connected. The formation of the pores originates from the dehydroxylation and is responsible for the transparency loss of the samples. In dense HAp ceramic

Table 2
The ratios of band intensities in the FTIR spectra of samples annealed at different temperatures.

Annealing temperature (°C)	OH^{-1}/PO_4^{3-} (3569/600 cm^{-1})	OH^{-1}/PO_4^{3-} (629/600 cm^{-1})
800	0.068	0.531
900	0.067	0.529
1000	0.064	0.528
1100	0.058	0.520

Please cite this article in press as: Liu Y, Shen Z. Dehydroxylation of hydroxyapatite in dense bulk ceramics sintered by spark plasma sintering. *J. Eur. Ceram. Soc.* (2012), doi:10.1016/j.jeurceramsoc.2012.02.025

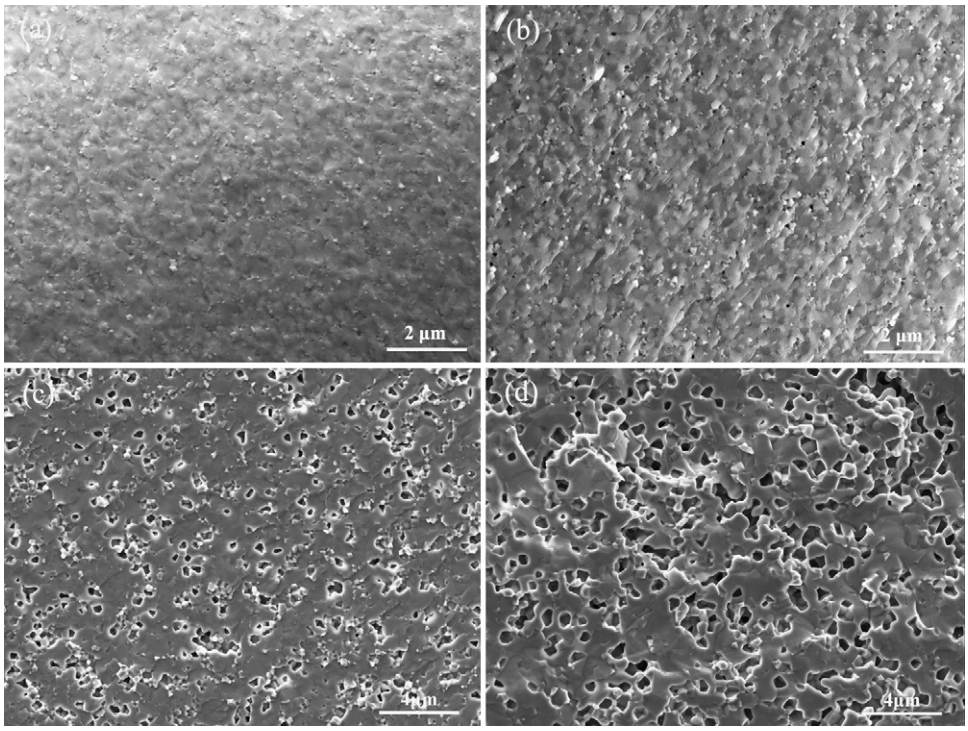

Fig. 6. Microstructures inside the samples annealed at (a) 800 °C, (b) 900 °C, (c) 1000 °C and (d) 1100 °C.

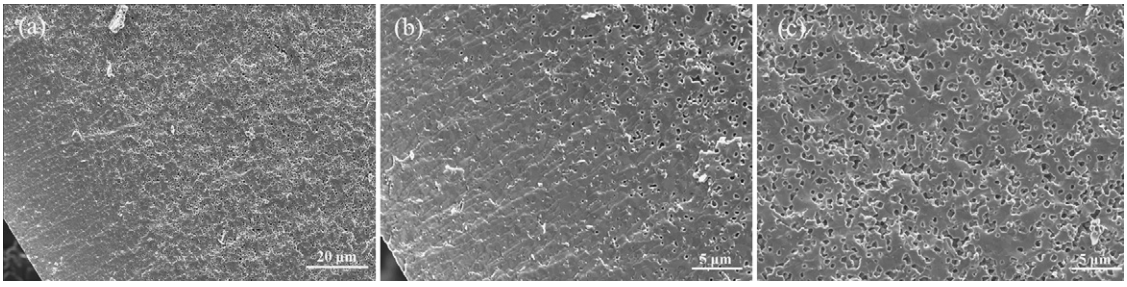

Fig. 7. Microstructures annealed at 1100 °C. (a) overview of cross-section, (b) near surface and (c) interiors.

samples, once dehydroxylation takes place, the released water vapour is trapped inside close pores. The water vapour is taken up later by the HAp lattice by rehydration during cooling, leaving in situ formed pores behind. Therefore, the distribution and the sizes of pores are dependent on the water vapour aggregation in the HAp ceramic samples. With the increase of annealing temperature more water vapour is released on one hand and the grains grow bigger on the other hand. The combination of these two effects results in the coalescence of water vapour and finally, more water vapour is aggregated in the local area and more pores are remaining in the HAp ceramic samples after cooling, as revealed by the microstructure features shown in Fig. 6.

Since the formation of the pores is related to the locally aggregated water vapour, few pores are observed near the surface layer of HAp ceramic samples where the water vapour is easy to diffuse away. A typical microstructure feature of the fracture surface across the annealed samples is shown in Fig. 7. It is evident that a structural gradient with porous interiors and denser surface layer is formed. It is intriguing to observe that a dense microstructure can still be achieved in the surface layer despite the water loss occurring during thermal annealing. This opens up the possibility to prepare artificial bones made of HAp that mimic the microstructure of nature bones consisting of compact and spongy components.

The pore formation during thermal annealing of dense HAp ceramics can be described as an anti-densification process in opposition to the densification by sintering. During the conventional sintering of HAp ceramics, if the water vapour is trapped inside the closed pores in the last stage of sintering, one obtains a similar microstructure as shown in Fig. 6(c). Further densification is inhibited by the formation of such filled pores by water vapour. The evidence shown by Fig. 7(b) that a dense microstructure can still be obtained as long as the water vapour can diffuse away indicate that any method enabling the decrease of the water vapour content in isolated pores can improve the densification of HAp ceramics.

3.4. The surface water vapour escaping patterns

Fig. 8 shows the surface topography of the thermal annealed HAp ceramic samples. It should be mentioned that the surfaces of all the samples are polished before annealing. Therefore, the

Please cite this article in press as: Liu Y, Shen Z. Dehydroxylation of hydroxyapatite in dense bulk ceramics sintered by spark plasma sintering. *J. Eur. Ceram. Soc.* (2012), doi:10.1016/j.jeurceramsoc.2012.02.025

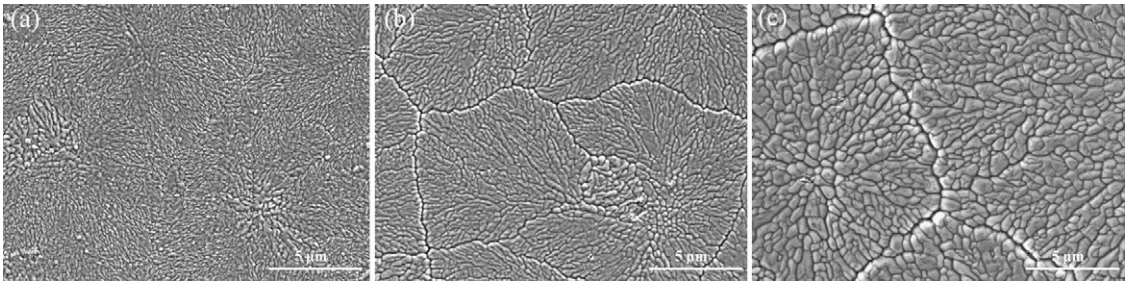

Fig. 8. Surface topographic structures of the samples annealed at (a) 900 °C, (b) 1000 °C and (c) 1100 °C.

observed surface topography reflects the water vapour escaping paths and the result of thermal etching. It can be seen that the grains on the surface layer show peculiar morphologies and patterns which is unusual for a normal thermal etching process. The water vapours trapped immediately beneath the surface have the shortest diffusion path towards top surface. They may aggregate firstly before escape by diffusion, leaving behind the water escaping patterns observed on the surface.

4. Conclusions

Fully dense transparent HAp ceramic samples almost free from dehydroxylation were prepared by spark plasma sintering at a minimized temperature. Further post-SPS thermal annealing carried out in air revealed a density decrease accompanied with no weight loss. It is concluded that no decomposition taking place in fully densified HAp ceramic samples by thermal annealing up to 1100 °C, whereas discernable dehydroxylation of HAp starts above 900 °C that yields the formation of pores and the volume expansion, i.e. an anti-densification process. The dehydroxylation of HAp at high temperature makes the in situ formation of pores and a gradient structure composed of porous interior and dense surface layer across entire HAp ceramic samples. The dense surfaces of the annealed samples demonstrate a peculiar topography reflecting the water vapour escaping patterns.

Acknowledgements

This work was supported by the Swedish Governmental Agency for Innovation Systems (Vinnova) and the Swedish Research Council (VR) through the Berzelii centre EXSELENT on porous materials. The support of the Knut and Alice Wallenberg foundation for the purchase of electron microscopes used in this study is gratefully acknowledged.

References

1. Hench LL. Bioceramics. *J Am Ceram Soc* 1998;**81**:1705–28.
2. Suchanek W, Yoshimura M. Processing and properties of hydroxyapatite-based biomaterials for use as hard tissue replacement implants. *J Mater Res* 1998;**13**:94–117.
3. Sun LM, Berndt CC, Gross KA, Kuckuk A. Material fundamentals and clinical performance of plasma-sprayed hydroxyapatite coatings: a review. *J Biomed Mater Res* 2001;**58**:570–92.
4. Kong YM, Bae CJ, Lee SH, Kim HW, Kim HE. Improvement in biocompatibility of ZrO_2–Al_2O_3 nano-composite by addition of HA. *Biomaterials* 2005;**26**:509–17.
5. Shen ZJ, Adolfsson E, Nygren M, Gao L, Kawaoka H, Niihara K. Dense hydroxyapatite–zirconia ceramic composites with high strength for biological applications. *Adv Mater* 2001;**13**:214–6.
6. Shi SL, Pan W, Fang MH, Fang ZY. Reinforcement of hydroxyapatite bioceramic by addition of Ti_3SiC_2. *J Am Ceram Soc* 2006;**89**:743–5.
7. Rapacz-Kmita A, Slosarczyk A, Paszkiewicz Z. Mechanical properties of HAp-ZrO_2 composites. *J Eur Ceram Soc* 2006;**26**:1481–8.
8. Cihlar J, Buchal A, Trunec M. Kinetics of thermal decomposition of hydroxyapatite bioceramics. *J Mater Sci* 1999;**34**:6121–31.
9. Gross KA, Berndt CC, Stephens P, Dinnebier R. Oxyapatite in hydroxyapatite coatings. *J Mater Sci* 1998;**33**:3985–91.
10. Wang T, Dorner-Reisel A, Müller E. Thermogravimetric and thermokinetic investigation of the dehydroxylation of a hydroxyapatite powder. *J Eur Ceram Soc* 2004;**24**:693–8.
11. Wang T, Dorner-Reisel A, Müller E. Thermo-analytical investigations of the decomposition of oxyhydroxyapatite. *Mater Lett* 2004;**58**:3025–8.
12. Liao CJ, Lin FH, Chen KS, Sun JS. Thermal decomposition and reconstitution of hydroxyapatite in air atmosphere. *Biomaterials* 1999;**20**:1807–13.
13. Locardi B, Pazzaglia UE, Gabbi C, Profilo B. Thermal behaviour of hydroxyapatite intended for medical applications. *Biomaterials* 1993;**14**:437–41.
14. Hartmann P, Jäger C, Barth St, Vogel J, Meyer K. Solid state NMR, X-ray diffraction, and infrared characterization of local structure in heat-treated oxyhydroxyapatite microcrystals: an analogy of the thermal decomposition of hydroxyapatite during plasma-spray procedure. *J Solid State Chem* 2001;**160**:460–8.
15. Dorozhkin SV. Bioceramics of calcium orthophosphates. *Biomaterials* 2010;**31**:1465–85.
16. Mazaheri M, Haghighatzadeh M, Zahedi AM, Sadrnezhaad SK. Effect of a novel sintering process on mechanical properties of hydroxyapatite ceramics. *J Alloys Compd* 2009;**471**:180–4.
17. Wang JW, Shaw LL. Morphology-enhanced low-temperature sintering of nanocrystalline hydroxyapatite. *Adv Mater* 2007;**19**:2364–9.
18. Kalita SJ, Verma S. Nanocrystalline hydroxyapatite bioceramic using microwave radiation: synthesis and characterization. *Mater Sci Eng C* 2010;**30**:295–303.
19. Ramesh S, Tan CY, Bhaduri SB, Teng WD. Rapid densification of nanocrystalline hydroxyapatite for biomedical applications. *Ceram Int* 2007;**33**:1363–7.
20. Veljović Dj, Jokić B, Petrović R, Palcevskis E, Dindune A, Mihailescu IN, et al. Processing of dense nanostructured HAP ceramics by sintering and hot pressing. *Ceram Int* 2009;**35**:1407–13.
21. Guo XY, Xiao P, Liu J, Shen ZJ. Fabrication of nanostructured hydroxyapatite via hydrothermal synthesis and spark plasma sintering. *J Am Ceram Soc* 2005;**88**:1026–9.
22. Fujimori H, Toya H, Ioku K, Goto S, Yoshimura M. In situ observation of defects in hydroxyapatite up to 1200 °C by ultraviolet Raman spectroscopy. *Chem Phys Lett* 2000;**325**:383–8.
23. Rey C, Collins B, Goehl T, Dickson IR, Glimcher MJ. The carbonate environment in bone mineral: a resolution enhanced Fourier transform infrared spectroscopy study. *Calcif Tissue Int* 1989;**45**:157–64.

Please cite this article in press as: Liu Y, Shen Z. Dehydroxylation of hydroxyapatite in dense bulk ceramics sintered by spark plasma sintering. *J. Eur. Ceram. Soc.* (2012), doi:10.1016/j.jeurceramsoc.2012.02.025